Manuscript
Click here to access/download;Manuscript;Adsorption of RNZ and DFC GACs ESPR Yellow Highligthed.docx
Click here to view linked References

SINGLE ADSORPTION OF DICLOFENAC AND RONIDAZOLE FROM AQUEOUS SOLUTION ON COMMERCIAL ACTIVATED CARBONS: EFFECT OF CHEMICAL AND TEXTURAL PROPERTIES

Adriana I. Moral-Rodríguez[1], Roberto Leyva-Ramos[1]*, Esmeralda Mendoza-Mendoza[1,2], Paola E. Díaz-Flores[3], Damarys H. Carrales-Alvarado[4], María F. Alexandre-Franco[5], Carmen Fernández-González[5]

[1] Centro de Investigación y Estudios de Posgrado, Facultad de Ciencias Químicas, UASLP, Av. Dr. Manuel Nava No. 6, San Luis Potosí, SLP 78210, Mexico

[2] Cátedra-CONACYT

[3] Facultad de Agronomía y Veterinaria, Universidad Autónoma de San Luis Potosí. San Luis Potosí, SLP 78321, Mexico

[4] Instituto de Catálisis y Petroleoquímica, CSIC, C/Marie Curie 2, L10, 28049 Madrid, Spain.

[5] Departamento de Química Orgánica e Inorgánica, Universidad de Extremadura, Badajoz, Spain

*Corresponding author: E-mail: rlr@uaslp.com

ABSTRACT

The importance of the textural and physicochemical characteristics upon the adsorption capacity of the commercial activated carbons (ACs) Coconut, Wood, Merck, Darco and Norit towards ronidazole (RNZ) and diclofenac (DCF) from water solution was investigated thoroughly in this work. At pH = 7, Coconut AC and Wood AC presented the highest adsorption capacity towards RNZ (444 mg/g) and DCF (405 mg/g). The maximum mass of RNZ adsorbed onto Coconut AC was higher in this study than those outlined previously in other works. Besides, the maximum capacity of Wood AC for adsorbing DCF was comparable to those found for other ACs. The adsorption capacity of all the ACs was increased by surface area and was favored by incrementing the acidic site concentration. The π-π stacking interactions were the predominant adsorption mechanism for the RNZ and DCF adsorption on ACs, and the acidic sites favored the adsorption capacity by activating the π-π stacking. Electrostatic interactions did not influence the adsorption of RNZ on Coconut AC, but electrostatic repulsion decreased that of DCF on Wood AC. The adsorption of DCF on Wood AC was reversible but not that of RNZ on Coconut AC. Besides, the adsorption of RNZ and DCF on the Coconut and Wood ACs was endothermic in the range of 15-25 °C.

Keywords: Activated carbon, adsorption mechanism, diclofenac, ronidazole, surface chemistry.

1. INTRODUCTION

The excessive utilization of pharmaceuticals in animal and human health care has originated that considerable amounts of drugs are being discharged to the aquatic environment (surface, drinking and ground waters), sediments, soil, and food chains (Wang and Wang 2016). Effluents from municipal wastewater treatment plants release pharmaceutical compounds into surface water sources since the existing biological water treatment processes do not successfully remove these compounds. Antibiotics and anti-inflammatories are some of the most commonly detected organic microcontaminants in municipal wastewater, posing a disturbing hazard since these compounds are toxic even at trace levels (Halling-Sørensen et al. 1998; Jeon and Hollender 2019; Ternes and Hirsch 2000).

Antibiotics are broadly prescribed to prevent or treat microbial infections, and several of them are recalcitrant or difficult to decompose in aerobic biological treatment processes (Kümmerer 2009). Distinct antibiotics were found in the hospital residual waters, industrial and municipal wastewater and surface water. Amoxicillin (900-9940 ng/L) (Watkinson et al. 2009), ampicillin (5800 ng/L) (Lin et al. 2008), cephalexin (3100-64000 ng/L) (Watkinson et al. 2009), ciprofloxacin (11-15000 ng/L) (Spongberg and Witter 2008; Watkinson et al. 2009), sulfamethoxazole (4-9460 ng/L) (Díaz-Cruz et al. 2008) and tetracycline (15000 ng/L) (Lin et al. 2008) are some of the antibiotics detected in water resources.

Notwithstanding, the nonsteroidal anti-inflammatory pharmaceuticals (NSAIDs) are being widely prescribed for curing dysmenorrhea fever, headaches, inflammatory arthropathy, osteoarthritis and rheumatoid arthritis, among others (Richard et al. 2007). These anti-inflammatories have been found not only in surface waters but also in residual waters. Among the NSAIDs frequently detected in water are acetaminophen (211 ng/L)

(Santos et al. 2013), diclofenac (60-1900 ng/L) (Gómez et al. 2007), famotidine (94 ng/L) (Lin et al. 2008) and ibuprofen (300 ng/L) (Lin and Tsai 2009).

Various processes have been applied to eliminating pharmaceutical compounds in water. Among these, advanced oxidation processes, adsorption, photodegradation, soil sorption, electrochemical degradation and biosorption by aquatic plants are being successfully applied lately (Chianese et al. 2016; Moral-Rodriguez et al. 2016; Martínez-Costa et al. 2020).

Adsorption is a separation process that has attracted considerable attention due to the low operating costs and availability of different adsorbents. Different activated carbons (ACs) have been prepared for removing various drugs from water solutions. Malhotra et al. (Malhotra et al. 2018) examined the adsorption of diclofenac (DCF) on an AC synthesized by chemical activation of tea residues using $ZnCl_2$, K_2CO_3, KOH and H_2SO_4, denoted as AC1, AC2, AC3 and AC4, correspondingly. The adsorption capacity decreased in the following order: AC1 > AC2 > AC3 > AC4; likewise, the surface diminished in the same order.

Recently, the adsorption capacity of a commercial AC towards DCF was enhanced by modifying the commercial AC using chemical activation with CO_2, and the adsorption capacity was raised nearly linearly with the AC surface area (Moral-Rodríguez et al. 2019). In another work, ACs were synthesized from sewage sludge that was mixed with a $ZnCl_2$ solution, using different ratios of $ZnCl_2$/sludge (0.5, 1.0, and 1.5) and carbonized at different temperatures (500, 650 and 800 °C) (dos Reis et al. 2016). These ACs were applied to remove nimesulide (NM) and DCF in a water solution, and the maximum mass of NM and DCF adsorbed was 66.4 and 157.4 mg/g, correspondingly.

Moral-Rodríguez et al. (2016) researched for eliminating ronidazole (RNZ) and sulfamethoxazole (SMX) from a water solution by adsorption on a commercial AC, designated as F400. The findings disclosed that the adsorption of SMX on F400 relied on the temperature, ionic strength, pH and aqueous matrix, whereas the operating conditions did not change the adsorption of RNZ on F400. Furthermore, the uptake of RNZ adsorbed on F400 was higher (352.26 - 518.39 mg/g) than that of SMX (126.64 - 445.77 mg/g). It was also demonstrated that the F400 capacity towards RNZ and SMX was significantly dependent upon its textural properties and the molecular size of each antibiotic.

Although the effectiveness of adsorption on carbonaceous materials for eliminating pharmaceutical compounds in aqueous solution has been extensively analyzed. The novelty of this work is to study the relationship between the adsorption capacity of activated carbon and their chemical and textural properties. Therefore, this study's principal goal was to analyze the adsorption equilibrium of DCF and RNZ on five commercial ACs having different chemical and textural characteristics. Besides, the dependence of the adsorption capacities of these ACs regarding solution pH and temperature was investigated in detail. Moreover, the adsorption mechanisms of RNZ and DCF on the ACs were explained and the reversibily of the adsorption and reuse of ACs were also examined in this work.

2. EXPERIMENTAL METHODOLOGY

2.1 Adsorbents and characterization

Five commercial ACs were used and were designated as Coconut, Wood, Merck, Darco and Norit. The ACs were pretreated by washing with water, drying in an electric oven overnight (T = 120 °C), sieving and storing in a sealed vessel. The particles of ACs have a mean diameter of 0.056 mm.

115 The textural properties of ACs, namely surface area (S_{BET}), pore volume (V_P), and
116 average pore diameter (d_P), were assessed from the adsorption-desorption isotherm of N_2,
117 which was measured in a physisorption apparatus, Micromeritics, ASAP 2020. The
118 determination of S_{BET} was carried out by the method proposed by Brunauer, Emmett, and
119 Teller (BET) (Brunauer et al. 1938). The Dubinin-Radushkevich (DR) isotherm (Rouquerol
120 et al. 2014) was applied to evaluate the micropore volume (V_{mic}), specific micropore area
121 (S_{mic}) and average micropore width (L_0). Lastly, the pore size distribution of each AC was
122 computed using the density functional theory. The basic and acidic sites concentrations on
123 the AC surface were ascertained by Boehm's titration method (Boehm 1966); otherwise, the
124 surface charge of the adsorbents was assessed by the acid-base titration technique developed
125 by Babic et al. (1999).

126 **2.2 Technique for procuring the adsorption data of RNZ and DCF**

127 The pharmaceutical compounds employed in this study were ronidazole (RNZ) and
128 diclofenac sodium (DCF), supplied by Merck. Table 1 displays the chemical characteristics
129 and molecular structure of RNZ and DCF. The molecular structure of each compound was
130 obtained by applying the hybrid density functional b3lyp. Fig. 1a and 1b show the speciation
131 diagrams for RNZ and DCF in water solutions, calculated using the corresponding
132 dissociation constants (see Table 1).

133 The determination of RNZ and DCF was performed by UV-Visible
134 spectrophotometry. The calibration curves for RNZ and DCF were prepared from standard
135 solutions having concentrations from 100 to 1000 mg/L. A spectrophotometer, Shimadzu
136 (model UV 2600), was employed to determine the absorbances of RNZ and DCF solutions
137 at wavelengths of 309 and 276 nm, correspondingly, and the calibration curves were made at
138 the particular pH of the RNZ and DCF sample solutions.

A solution with an ionic strength (0.01 N) and a specific pH was fixed by combining appropriate volumes of 0.01 N HCl and NaOH solutions. This constant ionic strength solution was employed for fixing all RNZ and DCF solutions, having initial concentrations varying from 100 to 1000 mg/L.

The data for the RNZ and DCF adsorption on the ACs were obtained in an experimental adsorber operated in batch mode. An AC mass of 50 mg and 40 mL of the RNZ or DCF solutions of different initial concentrations were added into 50 mL Falcon tubes (adsorber). Afterward, the Falcon tube was set down in a thermostatic bath, allowing the solution and ACs to reach adsorption equilibrium. In preliminary tests, the concentration of the pharmaceuticals in solution was monitored daily, and the concentration did not change after 5 days so that 7 days was sufficient time to approach equilibrium. Three times daily, the adsorber solutions were mechanically shaken for 15 min by placing the adsorbers on top of an Orbital Shaker TS-100. Posterior to 7 days, a solution was taken out and analyzed by the analytical method detailed above to quantify the equilibrium concentration of the pharmaceutical.

At T = 25 °C, the dependence of the adsorption equilibrium on pH was analyzed by procuring the adsorption data at pH of 3, 7 and 11 for RNZ and pH of 6, 7, 9 and 11 for DCF. In all the experimental runs, few drops of HCl and NaOH solutions of 0.01 N were supplemented to keep the solution pH constant. Moreover, the temperature influence was analyzed by measuring the adsorption equilibrium data at 35, 25, and 15 °C and pH = 7. The mass adsorbed of RNZ and DCF on the carbons was appraised by conducting a mass balance of the pharmaceutical in the batch adsorber, expressed as follows:

$$q = \frac{V(C_0 - C_e)}{m} \quad (1)$$

Where q denotes the mass of RNZ or DCF adsorbed at equilibrium (mg/g), V represents the volume of the RNZ or DCF solutions (L), C_0 is the initial concentration of the RNZ or DCF (mg/L), C_e is the equilibrium concentration of RNZ or DCF (mg/L), and m is AC mass (g).

2.3 Technique for conducting the desorption and reuse experiments

The desorption and reuse experiments of the pharmaceutical compounds were evaluated by conducting an adsorption-desorption-re-adsorption cycle. Firstly, at T = 25 °C and I = 0.01 N, the adsorption of DCF on Wood AC at pH = 6 and RNZ on Coconut AC at pH = 7 were conducted as described above. The Wood and Coconut ACs were chosen because they presented the highest adsorption capacity towards DCF and RNZ. The AC equilibrated with the pharmaceutical compound was extracted from the solution, rinsed with 20 mL of deionized water for 5 min to remove the pharmaceutical not adsorbed, and the rinsing water was decanted. Then, AC was subsequently transferred into another adsorber holding a solution without the pharmaceutical compound (40 mL) with I = 0.01 N and pH = 11 for DCF and pH = 7 for RNZ. The pH was measured and adjusted periodically to keep it constant, as described above. Upon reaching desorption equilibrium (eight days), the solution was sampled, and the concentration of the pharmaceutical compound was determined as described above. The amount of pharmaceutical not desorbed was computed as follows:

$$q_{des,e} = q_o - \frac{V}{m} C_{des,e} \quad (2)$$

where $C_{des,e}$ is the concentration of the pharmaceutical compound at equilibrium in the desorption experiment, mg/L; q_o is the uptake of the pharmaceutical already adsorbed at the starting of the desorption experiment, mg/g; $q_{des,e}$ represents the equilibrium uptake of the pharmaceutical that did not desorb in the desorption run, mg/g.

After the desorption experiment, the AC was extracted from the solution, rinsed with deionized water as described previously and designated as regenerated AC. Then, the regenerated AC was added into a batch adsorber to perform an adsorption experiment, and the re-adsorption capacity of the regenerated AC, q_{ReAd}, was calculated by equation (1).

The re-adsorption efficiency (%RE) of the ACs for a new cycle of adsorption was calculated using the subsequent equation:

$$\%RE = \frac{q_{ReAd}}{q} \times 100\ \% \quad (3)$$

3. RESULTS AND DISCUSSION

3.1 Properties of Commercial ACs

The textural characteristics S_{BET}, V_P, d_P, V_{mic}, L_0, and S_{mic} of all ACs are registered in Table 2. The S_{BET} of the ACs decreased from 1357 to 510 m^2/g, and the decreasing order is as follows: Wood > Merck > Coconut > Norit > Darco. Furthermore, the total V_p was evaluated at $(P/P_s) = 0.99$ and varied from 0.44 to 1.18 cm^3/g, showing that the porosity of the ACs changed broadly.

The adsorption-desorption isotherms of N_2 on the ACs are plotted in Fig. S.1. According to the classification recommended by IUPAC (Rouquerol et al. 2014), the isotherm shapes of Coconut and Merck ACs are type Ia (Fig. S.1 a) and Ib (Fig. S.1 b), respectively. These isotherms are reversible and have a high opening in the adsorption shoulder, which is characteristic of microporous materials. For the isotherm Ia, the type of microporosity is narrower if compared to that of isotherm Ib, where the diameters of the micropores are wider according to the opening of the adsorption shoulder (see isotherm Ib). The adsorption isotherms of the Darco, Norit, and Wood ACs have shapes of type IIb (Fig.

S.1 c, d, and e), distinctive of mesoporous materials, showing the hysteresis loops H_3 and H_4 type. The hysteresis loop H_3 (Fig. S.1 c) often occurs in materials formed by aggregates of particles with sheet morphology, while the H_4 (Fig. S.1 d and e) is typical of activated carbons and other adsorbents, which have slit shape pores and high distribution of micropores (Boehm 1966).

The V_{mic} of the Coconut, Merck, Norit, Darco and Wood ACs represented 86, 58, 51, 36 and 34 % of the total V_p, respectively, confirming that the Coconut and Merck ACs consisted mainly of micropores.

Fig. S.2 displays the cumulative pore volume and distribution of pore size for all ACs. The accumulated pore volume distribution of the Coconut AC (see Fig. S.2 a) shows that the volume of micropores is 94.3 % of the entire pore volume, although the remaining 5.7 % is mesoporous. Furthermore, the pore size distribution is almost unimodal, and the approximate pore diameter was about 0.65 nm. Likewise, in Fig. S.2 e, the cumulative volume distribution of the Wood AC revealed that the micropores and mesopores represented 49 and 51 % of the total pore volume, correspondingly. On the other hand, it can be corroborated that most of the micropore sizes are between 0.5 and 0.75 nm for Coconut AC and varying from 0.65 to 0.75 nm for the Wood AC.

Table 3 shows that the concentrations of the total basic and acid sites for the ACs varied from 0.093 to 4.995 meq/g and 0.093 to 1.874 meq/g, respectively. As can be seen, the total acidic and basic sites concentrations ranged widely. The Wood AC surface exhibited a more acidic character (pH_{PZC} = 3.64), considering that the concentration of acidic sites was 7.7 times larger than that of the basic ones. Otherwise, the concentration of basic sites of Coconut AC was 7-fold larger than those of acid sites (pH_{PZC} = 10.85). In general, the acid sites concentrations of the ACs decreased as follows: Wood > Coconut > Norit > Darco >

228 Merck, whereas the basic sites diminished in the subsequent order: Coconut > Norit > Wood
229 > Merck ≈ Darco.

230 **3.2 Modeling the adsorption data of RNZ and DCF**

231 The adsorption isotherms of Freundlich, Langmuir and Prausnitz-Radke (P-R)
232 interpreted the data for the adsorption equilibrium of both pharmaceuticals. These isotherm
233 models are mathematically expressed as follows (Leyva-Ramos 2007):

$$q = kC^{\frac{1}{n}} \quad (4)$$

$$q = \frac{q_m KC}{1+KC} \quad (5)$$

$$q = \frac{aC}{1+bC^{\beta}} \quad (6)$$

234 Where *a* (L/g), *b* (L^{β}/mg^{β}) and β are the Prausnitz-Radke model constants, C (mg/L) denotes
235 the equilibrium concentration of pharmaceutical, k ($mg^{1-1/n}L^{1/n}/g$) and n designate the
236 Freundlich model constants, K (L/mg) and q_m (mg/g) are the Langmuir isotherm parameters
237 associated with the adsorption heat and the maximum mass of pharmaceutical adsorbed on
238 ACs, respectively, and q (mg/g) represents the equilibrium amount adsorbed of
239 pharmaceutical.

240 The parameters for adsorption isotherms were calculated by matching the adsorption
241 models to the data using a nonlinear regression method based upon the Rosenbrock-Newton
242 optimization algorithm. Besides, the average percent deviation for each adsorption model,
243 %D, was appraised using the succeeding mathematical relationship:

$$\%D = \left(\frac{1}{N} \sum_{i=1}^{N} \left| \frac{q_{exp} - q_{pred}}{q_{exp}} \right| \right) \times 100\ \% \quad (7)$$

244 Tables 4 and 5 list the parameters and %D for the P-R isotherm, and the parameters
245 and %D for the Langmuir and Freundlich isotherms are registered in Tables S1, S2 and S3.

The %D values for the R-P isotherm model were shorter than the %D values of the Freundlich and Langmuir adsorption models in 22 out of the 28 experimental conditions registered in Tables 4, 5, S1, S2 and S3. Therefore, the P-R model better interpreted the experimental data since it is a three-parameter isotherm, while the Langmuir and Freundlich isotherms are two-parameter adsorption models. The P-R adsorption model adequately represented the experimental data since the %D varied from 0.9 to 21.0 %.

3.3 Adsorption of RNZ and DCF on ACs

At T = 25 ºC and pH = 7, the isotherms of RNZ and DCF adsorbed on ACs are shown in Fig. 2a and 2b. As depicted in Fig. 2a, the capacities of ACs for adsorbing RNZ in water solution diminished as follows: Coconut > Wood > Norit > Merck > Darco. At the RNZ equilibrium concentration of 500 mg/L, the uptake of RNZ adsorbed (q_{500}) upon the Coconut, Wood, Norit, Merck and Darco is 434, 350, 283, 261 and 188 mg/g, respectively. It can be noted that Coconut and Darco presented the largest and lowest adsorption capacity towards RNZ. In Fig. 2b, it is observed that Wood had the highest adsorption capacity towards DCF. The q_{500} for DCF on the Wood, Merck, Coconut, Norit and Darco is 396, 248, 222, 182 and 166 mg/g, correspondingly, so that the AC capacities for adsorbing DCF decreased in the subsequent series: Wood > Merck > Coconut > Norit > Darco. It is worth mentioning that the S_{BET} values of ACs decreased in the same order as their adsorption capacities towards DCF (See Table 2).

In this work, the maximum uptake of RNZ adsorbed on Coconut AC was 444 mg/g at pH of 7 and T of 25 °C and was slightly larger than those presented in previous studies (Méndez-Díaz et al. 2010; Moral-Rodríguez et al. 2016). The maximum adsorption capacities of three commercial carbons towards RNZ ranged from 376 to 394 mg/g (Méndez-Díaz et al. 2010; Moral-Rodríguez et al. 2016). While the Wood AC presented the maximum uptake

of DCF adsorbed of 441 mg/g, which is within the range (47.12-1033 mg/g) found for the adsorption capacities of pristine and modified ACs (Moral-Rodriguez et al. 2019; Viotti et al. 2019).

Fig. 3 depicts the molar uptake of DCF and RNZ adsorbed for the concentration at equilibrium of 500 mg/g, Q_{500} (mmol/g), graphed vs. the BET surface area of the AC. It can be noticed that the capacity of ACs for DCF incremented approximately linearly by augmenting S_{BET} and this result was expected because the adsorption capacities of the ACs decreased in same order as the S_{BET}. In the case of RNZ, the capacity of ACs for adsorbing RNZ increased somehow linearly with surface area, except for the Coconut AC. The finding that the surface area affected the adsorption capacity corroborated that the π-π dispersive interactions were the predominant adsorption mechanism. These interactions are related to the π electrons of the aromatic ring of RNZ or DCF and the π electrons existing in the AC graphene planes and the S_{BET} is directly related to the AC graphene planes. The Coconut AC had the greatest adsorption capacity towards RNZ, but the Coconut AC did not have the highest S_{BET} and was the AC having the largest concentration of basic sites. This result demonstrated that the surface chemistry of ACs could also affect their adsorption capacity.

The molar Q_{500} of RNZ was always higher than that of DCF independently of the AC. This result can be ascribed to the molecular dimensions of RNZ (Table 1), which are shorter than those of DCF so that the RNZ molecules can access more micropores than the DCF molecules, and more adsorption sites are available for adsorbing RNZ.

The molar Q_{500} for RNZ and DFC vs. the concentration of acidic sites per unit surface area of AC (acidic sites/S_{BET}) are plotted in Fig. 4. Overall, the acidic sites concentration promoted the adsorption capacity of ACs. Except for Merck AC, the capacities of the ACs for adsorbing DCF were raised linearly by increasing the concentration of acidic sites. Again,

294 the Coconut AC exhibited the highest molar Q_{500} for RNZ, but this carbon did not have the
295 largest concentration of acidic sites. The acidic site concentration favored the AC adsorption
296 capacity because some of the acidic sites can activate the π-π dispersion interactions
297 (Carrales-Alvarado et al. 2014). The preceding results corroborated that the ACs adsorption
298 capacities towards RNZ and DCF from water solutions are significantly dependent on the
299 textural and chemical characteristics of ACs.

300 **3.4 Influence of pH on the capacity of Coconut AC for adsorbing RNZ**

301 The dependence of the Coconut AC capacity for RNZ on the pH is exhibited in Fig.
302 5, and the adsorption capacity rises marginally by augmenting the pH from 3 to 7; however,
303 at pH = 11, the adsorption of RNZ on Coconut AC was significantly enhanced when the
304 concentrations of RNZ at equilibrium were higher than 200 mg/L. For the RNZ concentration
305 of 300 mg/L, the RNZ uptakes at pH of 3, 7, and 11 were 364, 389, and 548 mg/g,
306 respectively. Therefore, the mass of RNZ adsorbed at pH = 11 was 1.5 and 1.4-fold higher
307 than those at pH of 3 and 7, respectively.

308 The above results can be rationalized according to the speciation diagram of RNZ
309 (Fig. 1), which indicates that in the pH range of 3-9, the RNZ molecule exists as the
310 undissociated species, and the surface of the Coconut AC is positively charged (pH_{PZC} =
311 10.85). Hence, in this pH range, the electrostatic interactions did not influence the adsorption
312 of RNZ, confirming that the RNZ is adsorbed on Coconut AC by π-π interactions mainly.
313 Although the surface of the Coconut AC is now slightly negatively charged at pH = 11, and
314 the RNZ is still present as the neutral species, corroborating that the electrostatic interactions
315 did not affect the RNZ adsorption. However, at pH = 11, the adsorption capacity increased
316 for concentrations higher than 100 mg/L. This increase was due to the reduction of the RNZ
317 solubility at basic pH since the solubility of non-polar organic compounds diminishes in the

presence of salts (Carrales-Alvarado et al. 2014). At pH = 11, the concentration of Na^+ ions is augmented because of the addition of NaOH solution to adjust the solution pH. Consequently, the hydrophobic interactions between the RNZ and the water favored the accumulation of RNZ on the the surface of the Coconut AC. Hence, the adsorption of RNZ en Coconut AC at pH = 11 is related to the π-π dispersive interactions and hydrophobic interactions.

3.5 Influence of pH on the capacity of Wood AC for adsorbing DCF

Fig. 6 illustrates the pH influence on the capacity of Wood AC for adsorbing DCF. The adsorption capacity diminished considerably and moderately by incrementing the pH from 6 to 9 and 9 to 11, correspondingly. None adsorption runs were performed at pH < 6 because the DCF solubility in water is low (Llinàs et al. 2007). For a DCF equilibrium concentration of 300 mg/L, the uptake of DCF adsorbed was 568, 353, 278 and 244 mg/g for the pH values of 6, 7, 9 and 11, correspondingly. The capacity of Wood AC at pH = 6 was 1.6, 2.0 and 2.3 times higher than those at pH of 7, 9 and 11.

The above behavior can be ascribed to the fact that the DCF molecules in water are the anionic species (DCF^-) in the pH span from 6 to 11, while the surface of Wood AC is negatively charged (pH_{PZC} = 3.64). Thus, the lessening of the adsorption capacity was associated with the increment of the electrostatic repulsion existing between the negatively charged surface of the Wood AC and anionic DCF^- because the negative charge of AC surface augments by raising the pH.

The influence of the electrostatic interactions in the DCF adsorption mechanism on Wood AC was further analyzed by carrying out adsorption runs at the solution ionic strengths of 0.01, 0.1 and 1.0 N (Moral-Rodriguez 2019). The results (not shown in this work) demonstrated that the capacity of Wood AC for adsorbing DCF increased while raising the

ionic strength. The ionic strength was varied by changing the NaCl concentration in the solution, so the Na^+ ions adsorb on the AC negative surface, balancing the negative charge of the AC and decreasing the repulsion between DCF^- and the Wood AC surface, enhancing the adsorption of DCF. This effect is known as the screening effect (Moreno-Castilla 2004).

3.6 Desorption of pharmaceutical compounds and reuse of regenated AC

The reversibility of the adsorption of RNZ on Coconut AC and DCF on Wood AC was investigated by performing adsorption and desorption experiments. The adsorption of RNZ on Coconut AC was at pH = 7, and the desorption step was at the same pH. The pH of the desorption step was not varied because the adsorption capacity of Coconut AC did not depend on the pH for equilibrium concentrations of RNZ less than 100 mg/g. In the case of DCF, the adsorption of DCF on Wood AC was carried out at pH = 6 and the desorption at pH = 11. These pH conditions were selected because the Wood AC exhibited the highest and lowest adsorption capacity at pH = 6 and pH = 11. The desorption equilibrium data of RNZ and DCF from the Coconut and Wood ACs are displayed in Figures 7a and 7b. The experimental data for adsorption and desorption steps are denoted by the letter A and D, respectively, and followed by the corresponding experiment number.

The desorption percentage, %Des, was assesed by the subsequent equation:

$$\%Des = \frac{q_o - q_{des,e}}{q_o - q_{des,rev}} \times 100\ \% \qquad (8)$$

where $q_{d,rev}$ is the uptake of pharmaceutical adsorbed at the desorption equilibrium supposing that the adsorption is reversible, mg/g. The adsorption could be considered reversible if the %Des was equal to 100 %. Contrarily, the adsorption would be irreversible when %Des was less than 100 %. The $q_{des,rev}$ was computed by solving the Langmuir isotherm and equation (2) representing the desorption mass balance.

Figure 7a displays that the desorption equilibrium data D3, D4 and D5 are above the adsorption isotherm at pH = 7, demonstrating that the adsorption of RNZ on Coconut is not reversible. The %Des of RNZ adsorbed on Coconut AC were 80, 71 and 72 % for the experiments D3, D4 and D5 so less than 29 % of RNZ did not desorb and remained adsorbed. This result reveals that one of the adsorption mechanisms of RNZ is not reversible.

The %Des of DCF adsorbed on Wood AC were 100 and 98 % for the experiments D1 and D2, correspondingly, and as shown in Figure 7b, the desorption experimental data D1 and D2 were on the adsorption isotherm at pH = 11. Thus, the adsorption of DCF on Wood AC was reversible, corroborating that the predominant adsorption mechanisms of DCF on Wood AC are the electrostatic attractions and the π-π dispersion interactions.

After the desorption experiment, the capacity of the regenerated ACs for adsorbing pharmaceuticals was evaluated to analyze the reuse of the regenerated ACs. The re-adsorption efficiency %RE was calculated employing equation (3) and ranged between 72 and 77 % for DCF adsorbed on Wood AC at pH = 6, whereas the %RE for RNZ adsorbed on Coconut AC varied from 17 to 22 % at pH = 7. Thus, the regeneration of the CAs saturated with the pharmaceutical was adequate for the Wood AC but not for Coconut AC. Another regeneration method, such as microwave or thermal treatment, has to be investigated.

3.7 Effect of temperature on the capacity of Coconut and Wood ACs for adsorbing RNZ and DCF

The influence of temperature on the uptake of RNZ and DCF adsorbed on Coconut and Wood ACs at pH = 7 is depicted in Fig. 8. For an RNZ equilibrium concentration of 400 mg/L (See Fig. 8a), the uptake of RNZ adsorbed on Coconut AC was promoted and non-influenced by incrementing the temperature from 15 to 25 °C and 25 to 35 °C, respectively. A comparable tendency was also noted for the adsorption of RNZ on an AC commercially

known as Filtrasorb 400 when the temperature varied from 10 to 40 °C (Moral-Rodríguez et al. 2016). The mass of RNZ adsorbed at 35, 25 and 15 °C was 408, 403 and 352 mg/g, correspondingly indicating that the capacity of Coconut AC increased 14.5 % when the temperature rose from 15 to 25 °C. Likewise, Fig. 8b shows that the adsorption of DCF was significantly influenced by increasing the temperature from 15 to 25 and slightly augmented from 25 to 35 °C. For a DCF concentration of 400 mg/g, the uptakes of DCF adsorbed were 363, 413 and 427 mg/g at 15, 25 and 35 °C. These outcomes verified that the adsorption capacity of Wood AC towards DCF was raised 14 % and 3.4 % while incrementing the temperature from 15 to 25 °C and 25 to 35 °C.

The isosteric adsorption heat, $(\Delta H_{ads})_q$, for RNZ and DCF, was estimated using the experimental data at 15 and 25 °C since the adsorption capacity varied in this temperature range. The $(\Delta H_{ads})_q$ was estimated employing the following equation (Leyva-Ramos 1989):

$$(\Delta H_{ads})_q = \frac{R \, Ln \frac{C_2}{C_1}}{\frac{1}{T_2} - \frac{1}{T_1}} \quad (4)$$

where $(\Delta H_{ads})_q$ is the isosteric adsorption enthalpy, J/mol; R is the gas law constant, 8.314 J/K mol; C_2 and C_1 are the equilibrium concentrations of the pharmaceutical at temperatures T_2 and T_1, correspondingly, and at the same mass of the pharmaceutical adsorbed at equilibrium (q), mg/L; T_2 and T_1 are the temperatures at the conditions 2 and 1, respectively, K.

The ΔH_{ads} was estimated to be 56.5 and 56.3 kJ/mol for the adsorption of RNZ on Coconut AC at q = 358 mg/g, and DCF on Wood AC at q = 372 mg/g, correspondingly. Thus, the adsorption of both pharmaceuticals was endothermic. It is worthwhile to mention that the ΔH_{ads} decreased drastically as the q was reduced because the experimental adsorption equilibrium data were overlapped for q less than 270 mg/g.

4. CONCLUSIONS

Coconut, Wood, Merck, Norit and Darco ACs presented different textural and physicochemical properties. The S_{BET} varied from 510 to 1357 m^2/g, and the cumulative volume of micropores ranged from 34 to 86 %. The Wood AC had an acid character, whereas the Coconut AC showed a basic character. The Coconut AC exhibited the highest adsorption capacity towards RNZ (444 mg/g), while the Wood AC showed the maximum mass of DFC adsorbed (405 mg/g) from water solutions.

The surface area, as well as the acid sites concentration, significantly influenced the adsorption capacity of all ACs, corroborating that the predominant adsorption mechanism was the π-π stacking interactions. Besides, in the pH span of 3-7, the electrostatic interactions did not affect the adsorption of RNZ on Coconut AC; however, the hydrophobic interactions favored the adsorption of RNZ at pH = 11. In contrast, the capacity of Wood AC for DCF was reduced by the electrostatic repellence occurring between the negatively charged surface of the AC and the anionic DCF.

The desorption results revealed that the adsorption of DCF on Wood AC was reversible, whereas that of RNZ on Wood AC was not. The uptake of RNZ adsorbed on Coconut AC and DCF adsorbed on Wood AC was lessened by diminishing the temperature from 25 to 15 °C; hence, the adsorption of RNZ and DCF was endothermic in this temperature range. However, it remained nearly constant, incrementing the temperature from 25 and 35 °C.

The adsorption on ACs is a feasible process for efficiently removing RNZ and DCF from aqueous solutions, but the textural and chemical properties must be considered in selecting the proper commercial AC.

ACKNOWLEDGMENT

E. Mendoza-Mendoza thanks for the financial support to CONACyT through the Catedras program, project No. 864. This study was financially supported by Fondo de Apoyo a la Investigación (FAI)-Universidad Autonoma de San Luis Potosi (UASLP), through grant No.: C20-FAI-10-27.27.

DECLARATIONS

Authors' contributions AIMR carried out data curation, methodology, investigation, writing-original draft preparation and visualization. RLR performed funding acquisition, investigation, project administration, supervision, methodology, writing, reviewing and editing. EMM accomplished conceptualization, supervision, methodology, writing, reviewing and editing. PEDF engaged in methodology, writing-original draft preparation and visualization. DHCA participated in data curation, methodology and writing-original draft preparation. MFAF carried out methodology, investigation and characterization of activated carbons. CFG performed methodology, investigation and characterization of activated carbons.

Availability of data and materials: Datasets used during the current study and supplementary data are available from the corresponding author on reasonable request.

Compliance with ethical standards

Ethics approval and consent to participate: Not applicable.

Consent for publication: No applicable.

Competing interests: The authors declare that they have no competing interests.

REFERENCES

Babić BM, Milonjić SK, Polovina MJ, Kaludierović BV (1999) Point of zero charge and intrinsic equilibrium constants of activated carbon cloth. Carbon. https://doi.org/10.1016/S0008-6223(98)00216-4

Boehm HP (1966) Chemical identification of surface groups. Adv Catal. https://doi.org/10.1016/S0360-0564(08)60354-5

Brunauer S, Emmett PH, Teller E (1938) Adsorption of gases in multimolecular layers. J Am Chem Soc. https://doi.org/10.1021/ja01269a023

Carrales-Alvarado DH, Ocampo-Pérez R, Leyva-Ramos R, Rivera-Utrilla J (2014) Removal of the antibiotic metronidazole by adsorption on various carbon materials from aqueous phase. J Colloid Interface Sci. https://doi.org/10.1016/j.jcis.2014.08.023

Chianese S, Iovino P, Canzano S et al (2016) Ibuprofen degradation in aqueous solution by using UV light. Desalin Water Treat. https://doi.org/10.1080/19443994.2016.1153908

Díaz-Cruz MS, García-Galán MJ, Barceló D (2008) Highly sensitive simultaneous determination of sulfonamide antibiotics and one metabolite in environmental waters by liquid chromatography-quadrupole linear ion trap-mass spectrometry. J Chromatogr A. https://doi.org/10.1016/j.chroma.2008.03.029

Dos Reis GS, Bin Mahbub MK, Wilhelm M et al (2016) Activated carbon from sewage sludge for removal of sodium diclofenac and nimesulide from aqueous solutions. Korean J Chem Eng. https://doi.org/10.1007/s11814-016-0194-3

Gómez MJ, Martínez Bueno MJ, Lacorte S et al (2007) Pilot survey monitoring pharmaceuticals and related compounds in a sewage treatment plant located on the Mediterranean coast. Chemosphere. https://doi.org/10.1016/j.chemosphere.2006.07.051

481 Halling-Sørensen B, Nors Nielsen S, Lanzky PF et al (1998) Occurrence, fate and effects of
482 pharmaceutical substances in the environment- A review. Chemosphere.
483 https://doi.org/10.1016/S0045-6535(97)00354-8
484 Jeon J, Hollender J (2019) In vitro biotransformation of pharmaceuticals and pesticides by
485 trout liver S9 in the presence and absence of carbamazepine. Ecotoxicol Environ Saf.
486 https://doi.org/10.1016/j.ecoenv.2019.109513
487 Kümmerer K (2009) Antibiotics in the aquatic environment - A review - Part I. Chemosphere.
488 https://doi.org/10.1016/j.chemosphere.2008.11.086.
489 Leyva- Ramos R (1989) Effect of temperature and pH on the adsorption of an anionic
490 detergent on activated carbon. J Chem Technol Biotechnol.
491 https://doi.org/10.1002/jctb.280450308
492 Leyva-Ramos R (2007) Importancia y aplicaciones de la adsorción en fase líquida. In:
493 Moreno-Piraján JM(ed) Sólidos porosos, Preparación, Caracterización y Aplicaciones.
494 Ediciones Uniandes, Bogotá, Colombia, pp 155-211.
495 Lin AYC, Yu TH, Lin CF (2008) Pharmaceutical contamination in residential, industrial, and
496 agricultural waste streams: Risk to aqueous environments in Taiwan. Chemosphere.
497 https://doi.org/10.1016/j.chemosphere.2008.08.027
498 Lin AYC, Tsai YT (2009) Occurrence of pharmaceuticals in Taiwan's surface waters: Impact
499 of waste streams from hospitals and pharmaceutical production facilities. Sci Total Environ.
500 https://doi.org/10.1016/j.scitotenv.2009.03.009
501 Llinàs A, Burley JC, Box KJ et al (2007) Diclofenac solubility: Independent determination
502 of the intrinsic solubility of three crystal forms. J Med Chem.
503 https://doi.org/10.1021/jm0612970

504 Malhotra M, Suresh S, Garg A (2018) Tea waste derived activated carbon for the adsorption
505 of sodium diclofenac from wastewater: adsorbent characteristics, adsorption isotherms,
506 kinetics, and thermodynamics. Environ Sci Pollut Res. https://doi.org/10.1007/s11356-018-
507 3148-y
508 Martínez-Costa JI, Maldonado Rubio MI, Leyva-Ramos R (2020) Degradation of emerging
509 contaminants diclofenac, sulfamethoxazole, trimethoprim and carbamazepine by bentonite
510 and vermiculite at a pilot solar compound parabolic collector. Catal Today.
511 https://doi.org/10.1016/j.cattod.2018.07.021
512 Méndez-Díaz JD, Prados-Joya G, Rivera-Utrilla J et al (2010) Kinetic study of the adsorption
513 of nitroimidazole antibiotics on activated carbons in aqueous phase. J Colloid Interface Sci.
514 https://doi.org/10.1016/j.jcis.2010.01.089
515 Moral-Rodríguez AI, Leyva-Ramos R, Ocampo-Pérez R et al (2016) Removal of ronidazole
516 and sulfamethoxazole from water solutions by adsorption on granular activated carbon:
517 equilibrium and intraparticle diffusion mechanisms. Adsorption.
518 https://doi.org/10.1007/s10450-016-9758-0
519 Moral-Rodríguez AI, Leyva-Ramos R, Ania CO et al (2019) Tailoring the textural properties
520 of an activated carbon for enhancing its adsorption capacity towards diclofenac from aqueous
521 solution. Environ Sci Pollut Res. https://doi.org/10.1007/s11356-018-3991-x
522 Moreno-Castilla C (2004) Adsorption of organic molecules from aqueous solutions on
523 carbon materials. Carbon. https://doi.org/10.1016/j.carbon.2003.09.022
524 Richard H.D, Mycek M.J, Harvey R.A, Champe P.C (2007) Lippincott's Illustrated Reviews:
525 Pharmacology. Lippincott Williams & Wilkins.
526 Rouquerol F, Rouquerol J, Sing KSW et al (2014) Adsorption by powders and porous solids:
527 Principles, methodology and applications. Academic Press, France.

528 Santos LHMLM, Gros M, Rodriguez-Mozaz S et al (2013) Contribution of hospital effluents
529 to the load of pharmaceuticals in urban wastewaters: Identification of ecologically relevant
530 pharmaceuticals. Sci Total Environ. https://doi.org/10.1016/j.scitotenv.2013.04.077
531 Spongberg AL, Witter JD (2008) Pharmaceutical compounds in the wastewater process
532 stream in Northwest Ohio. Sci Total Environ.
533 https://doi.org/10.1016/j.scitotenv.2008.02.042
534 Ternes TA, Hirsch R (2000) Occurrence and behavior of X-ray contrast media in sewage
535 facilities and the aquatic environment. Environ Sci Technol.
536 https://doi.org/10.1021/es991118m
537 Viotti PV, Moreira WM, dos Santos OAA et al. (2019) Diclofenac removal from water by
538 adsorption on Moringa oleifera pods and activated carbon: Mechanism, kinetic and
539 equilibrium study. J Clean Prod. https://doi.org/10.1016/j.jclepro.2019.02.129
540 Wang J, Wang S (2016) Removal of pharmaceuticals and personal care products (PPCPs)
541 from wastewater: A review. J. Environ. Manage. 182:620–640.
542 https://doi.org/10.1016/j.jenvman.2016.07.049.
543 Watkinson AJ, Murby EJ, Kolpin DW, Costanzo SD (2009) The occurrence of antibiotics in
544 an urban watershed: From wastewater to drinking water. Sci Total Environ.
545 https://doi.org/10.1016/j.scitotenv.2008.11.059
546

Table 1. Molecular structure and physicochemical properties of RNZ and DCF.

Compound	Molecular structure	Molecular Weight (g/mol)	Dimensions X, Y, Z (nm)	pK_{ow}	pK_a
Ronidazole $C_6H_8N_4O_4$ (RNZ)	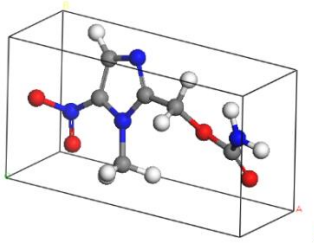	200.15	X: 0.913 Y: 0.448 Z: 0.264	0.38	pKa_1: 1.32 pKa_2: 12.99
Diclofenac sodium $C_{14}H_{10}Cl_2NNaO_2$ (DCF)	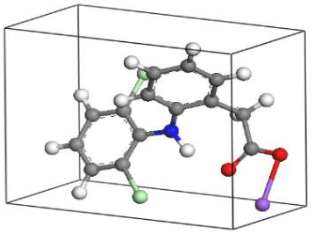	318.13	X: 0.960 Y: 0.708 Z: 0.472	3.91	pKa: 4.0

550 **Table 2.** Textural properties of the commercial ACs.

AC	S_{BET} (m^2/g)	V_P[a] (cm^3/g)	d_P[b] (nm)	V_{mic}[c] (cm^3/g)	L_0[d] (nm)	S_{mic} (m^2/g)
Wood	1357	1.18	3.51	0.40	1.41	746
Merck	1074	0.57	2.13	0.33	1.27	554
Coconut	960	0.44	1.81	0.38	0.97	800
Norit	646	0.55	3.43	0.28	0.93	433
Darco	510	0.58	5.34	0.21	1.22	328

551 [a] Total pore volumen

552 [b] Average pore diameter

553 [c] Micropore volume

554 [d] Micropore average width

555

556

557 **Table 3.** The concentration of acidic and basic sites of the commercial ACs.

Activated Carbon	Total acid sites (meq/g)	Total basic sites (meq/g)
Coconut	0.711	4.995
Merck	0.093	0.093
Darco	0.141	0.093
Norit	0.313	1.366
Wood	1.874	0.243

558

559

560

561 **Table 4.** Parameter values of the Prausnitz-Radke adsorption isotherms for the adsorption of
562 RNZ and DCF in aqueous solution on ACs at T = 25 ºC and pH = 7.

Compound	AC	a (L/g)	b (L^{β}/mg^{β})	β	%D
RNZ	Wood	50.3	0.46	0.81	3.7
	Merck	46.5	0.51	0.83	0.9
	Coconut	55.6	0.42	0.80	8.0
	Norit	165	1.26	0.89	4.4
	Darco	188	3.01	0.82	4.6
DCF	Wood	29.2	0.10	0.92	9.9
	Merck	104	1.30	0.82	10.5
	Coconut	709	6.70	0.88	14.1
	Norit	104	1.30	0.82	4.9
	Darco	5.41	0.05	0.90	1.8

563
564
565
566
567

568 **Table 5.** Parameters of the Prausnitz-Radke adsorption isotherms for the adsorption of RNZ
569 on Coconut and DCF on Wood from aqueous solution at different operating conditions and
570 I = 0.01 N.
571

Operating Conditions		RNZ on Coconut				DCF on Wood			
T (°C)	**pH**	***a*** **(L/g)**	***b*** **(Lβ/mgβ)**	**β**	**%D**	***a*** **(L/g)**	***b*** **(Lβ/mgβ)**	**β**	**%D**
25	6					114	0.26	0.95	15
25	7	55.6	0.42	0.80	8.0	29.2	0.10	0.92	9.9
25	9	313	2.55	0.78	21	36.3	0.17	0.94	1.4
25	11	27.9	0.20	0.75	2.5	119	1.15	0.84	3.1
15	7	84.2	0.63	0.84	9.0	22.7	0.23	0.78	19
35	7	167	1.34	0.80	1.0	23.7	0.06	0.97	2.0

572
573
574

List of Figure Captions

Fig. 1 Speciation diagrams of 1a) RNZ and 1b) DCF in aqueous solution as a function of the solution pH.

Fig. 2 Adsorption isotherms of a) RNZ and b) DCF at pH = 7 on ACs at T = 25 ºC and I = 0.01 N. The lines represent the predictions of the Radke-Prausnitz isotherm.

Fig. 3 Effect of surface area on the adsorption capacity of the ACs.

Fig. 4 Dependence of the adsorption capacity of ACs on the concentrations of the acidic sites per unit of surface area.

Fig. 5 Effect of solution pH on the adsorption isotherm of RNZ on Coconut AC at T = 25 °C and I = 0.01 N. The lines were predicted with the Radke-Prausnitz model.

Fig. 6 Effect of solution pH on the adsorption isotherm of DCF on Wood AC at T = 25 °C and I = 0.01 N. The lines show the prediction of the Radke-Prausnitz isotherm.

Fig. 7 Adsorption and desorption equilibrium data of pharmaceuticals on ACs at T = 25°C. a) Adsorption (pH = 7) and desorption (pH = 7) of RNZ on Coconut AC, and b) Adsorption (pH = 6) and desorption (pH = 11) of DCF on Wood AC. The lines represent the Radke-Prausnitz isotherm.

Fig. 8 Effect of temperature on the adsorption isotherms of a) RNZ on Coconut AC and b) DCF on Wood AC at pH = 7 and I = 0.01 N. The lines represent the isotherm of the Radke-Prausnitz model.

598

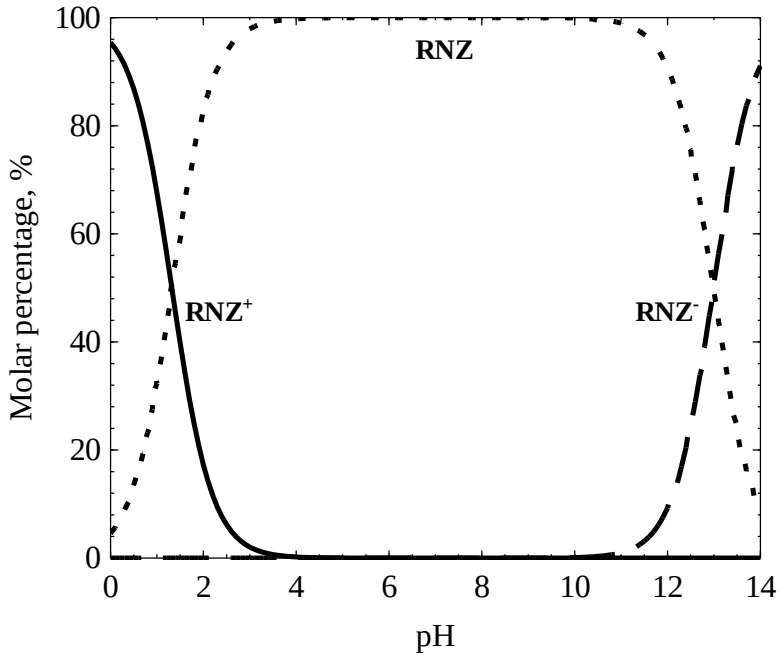

599 (a)

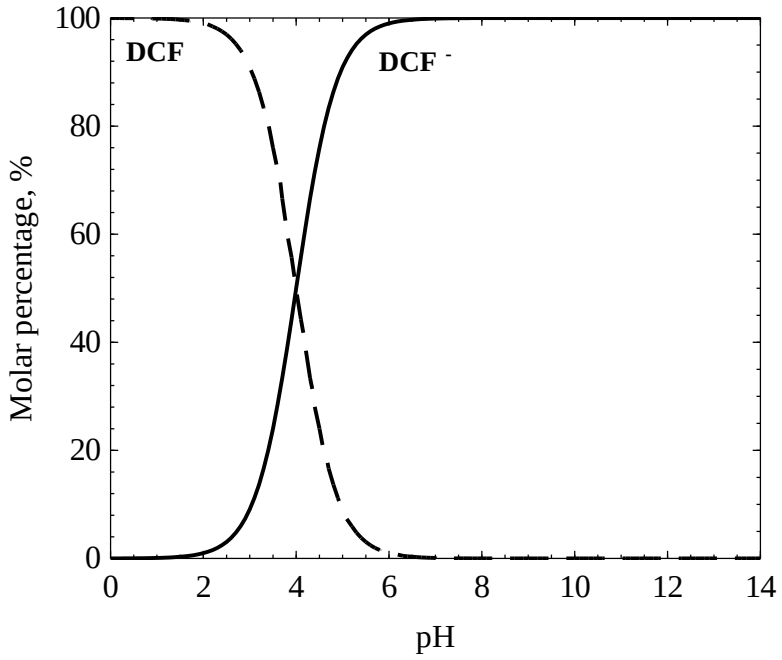

600 (b)

601 **Fig. 1**

602

603

604

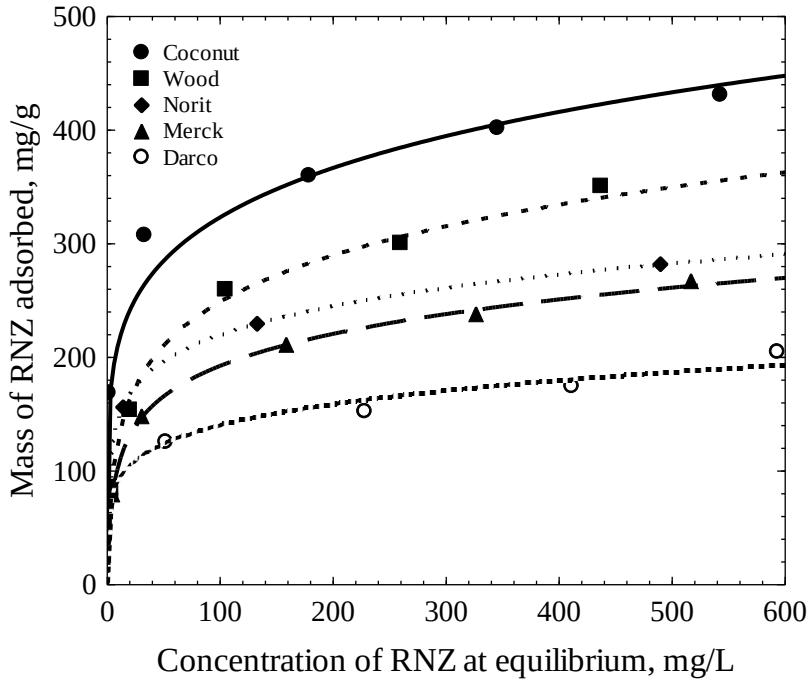

605 (a)

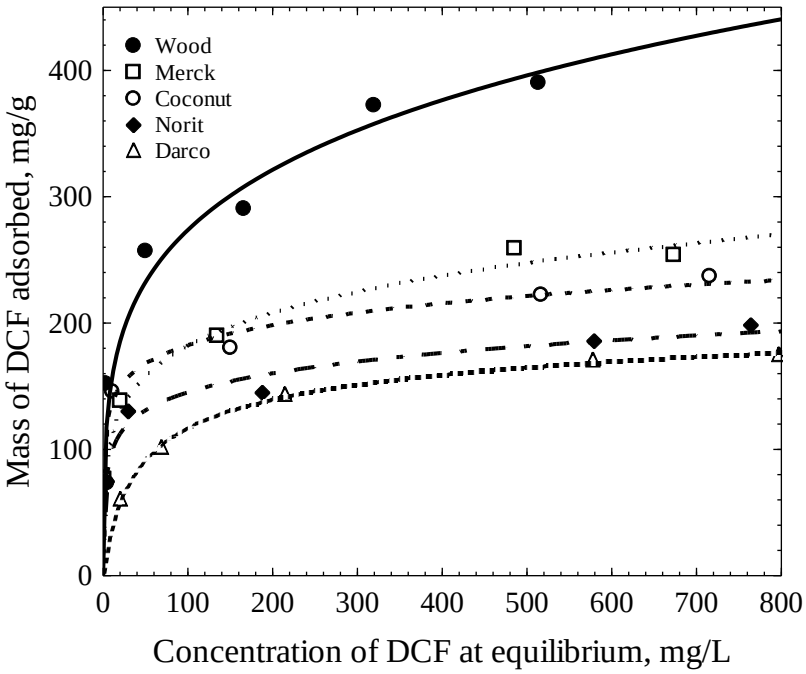

606 (b)

607 Fig. 2

608

609

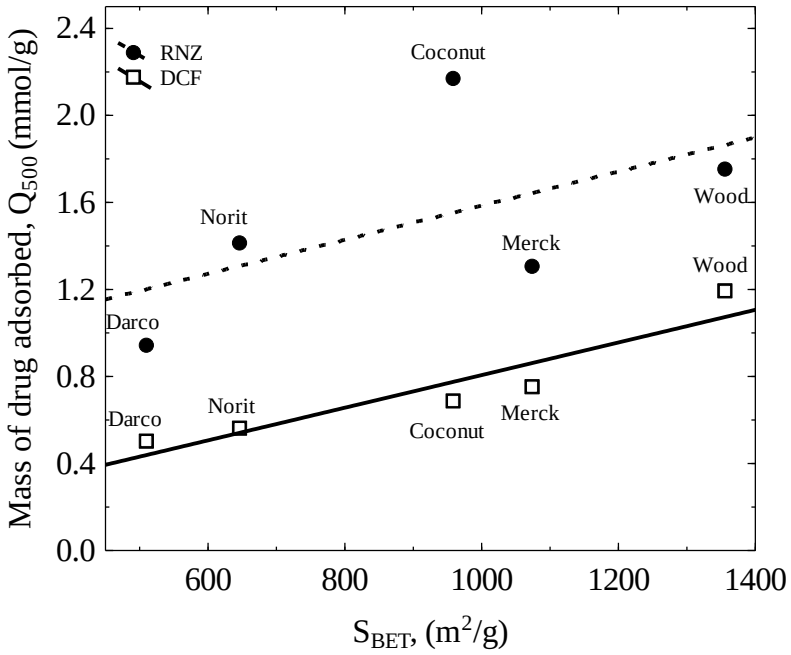

610

611 **Fig. 3**

612

613

614

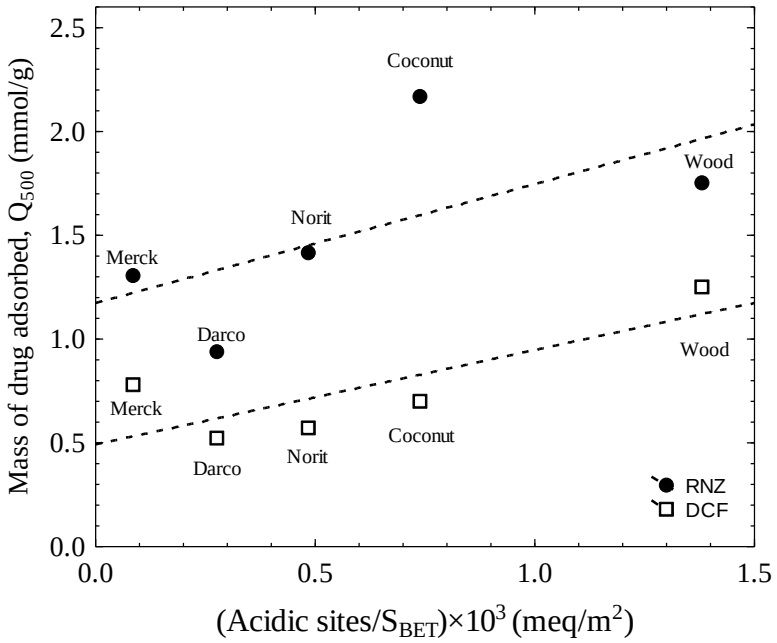

615

616

617 **Fig. 4**

618

619

620

621

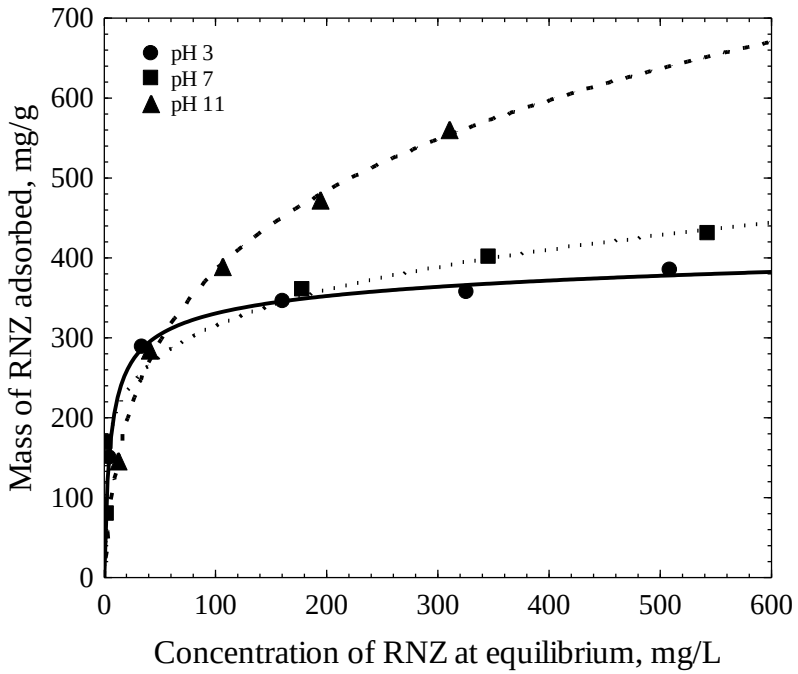

622

623 **Fig. 5**

624

625

626

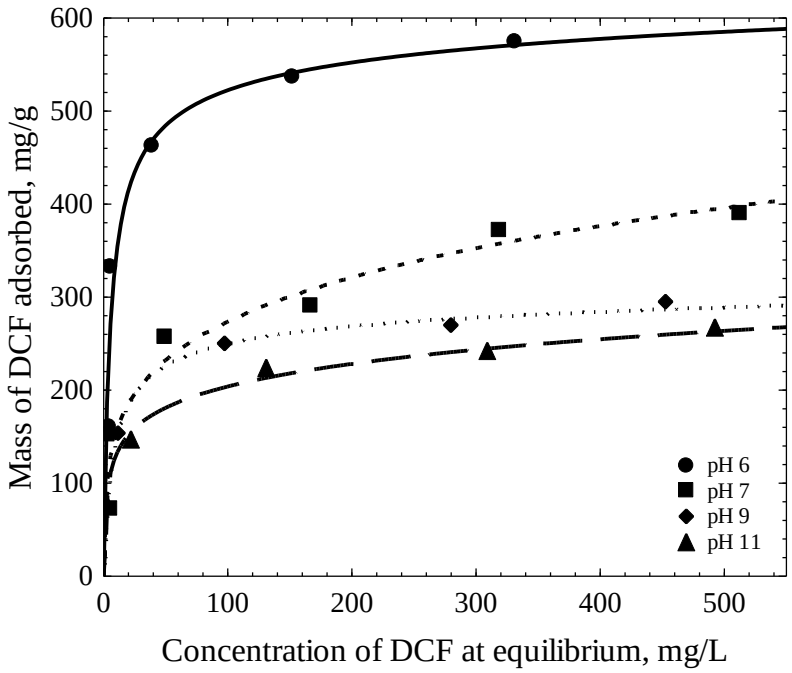

627

628 **Fig. 6**

629

630

631

632

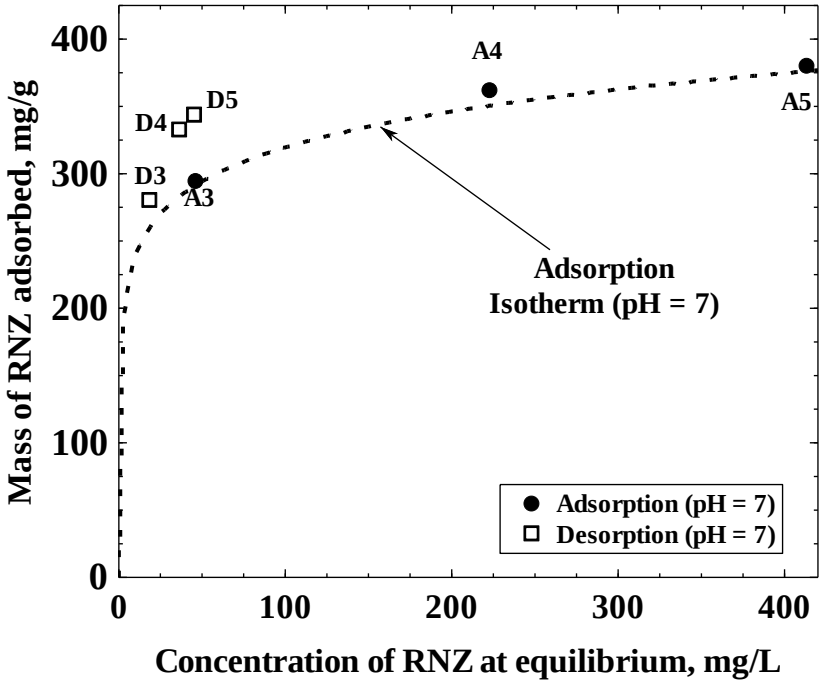

633 a)

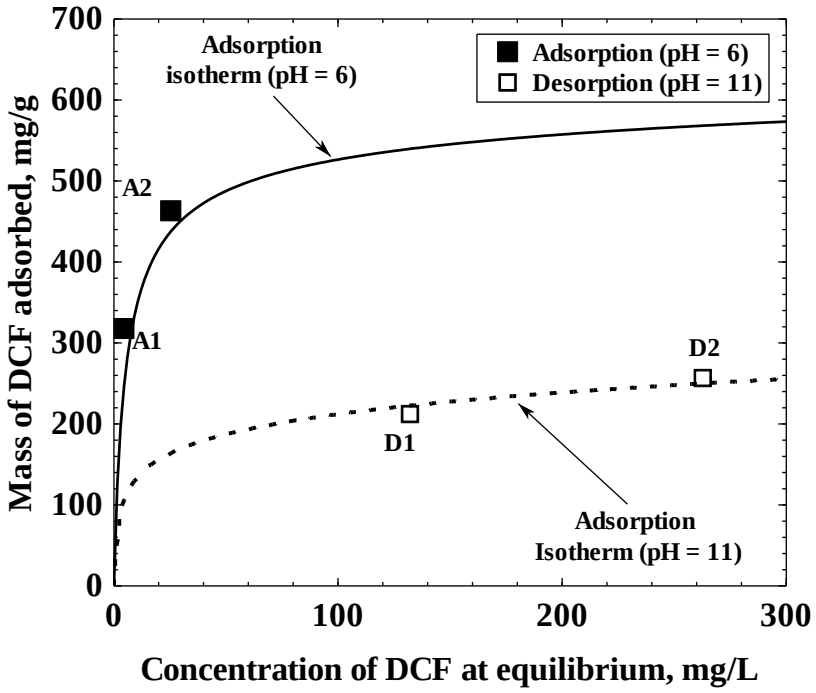

634 b)

635 **Fig. 7**

636

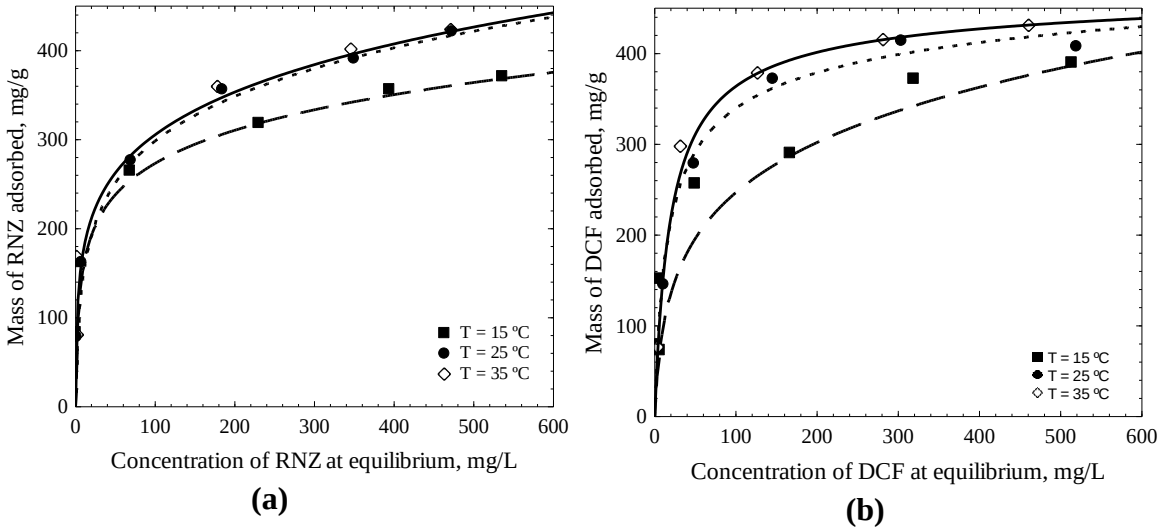

637

638 **Fig. 8**

639

640